Search for light WIMP recoils on methane with NEWS-G

Francisco A. Vazquez de Sola Fernandez⋆ on behalf of the NEWS-G collaboration

SUBATECH, IMT-Atlantique/CNRS-IN2P3/Université de Nantes, Nantes, 44307, France

⋆ vazquez@subatech.in2p3.fr

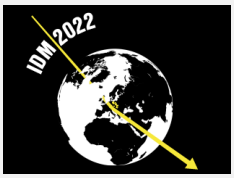

14th International Conference on Identification of Dark Matter
Vienna, Austria, 18-22 July 2022
doi:10.21468/SciPostPhysProc.12

Abstract

The NEWS-G collaboration is searching for light dark matter using single-electron-threshold Spherical Proportional Counters (SPCs) filled with light gaseous targets (H, He, Ne). NEWS-G has built a new 140 cm diameter SPC equipped with a multi-anode ACHINOS sensor. Robust calibrations with a UV laser and an ^{37}Ar source were performed to characterize the detector response to low energy events and achieve statistical background rejection. This work presents preliminary results from physics data taken with methane, leading to world-leading spin-dependent sensitivity under 2 GeV/c^2 WIMP masses.

Copyright F. A. Vazquez de Sola Fernandez.
This work is licensed under the Creative Commons
Attribution 4.0 International License.
Published by the SciPost Foundation.

Received 02-10-2022
Accepted 24-04-2023
Published 04-06-2024
doi:10.21468/SciPostPhysProc.12.073

Check for updates

1 Introduction

Astrophysical observations, from cosmological to galactic scales, strongly suggest the existence of invisible Dark Matter in our Universe [1, 2]. Weakly Interacting Massive Particles (WIMPs) are a category of Dark Matter candidates predicted by various extensions to the Standard Model [3]. The NEWS-G collaboration (New Experiments With Spheres - Gas) uses Spherical Proportional Counters (SPCs) to search for WIMPs. The kinematic match between light targets, such as neon or hydrogen, and light WIMPs is exploited to reach sensitivities to masses below 1 GeV/c^2, as demonstrated with the SEDINE prototype [4]. SPCs have also been used to test other physics models, such as solar KK axions [5]. This work describes the preliminary WIMP constraints obtained with a subset of the physics data taken with CH_4 inside the S140, the new generation SPC detector [6], while at Laboratoire Souterrain de Modane (LSM) [7].

2 S140 detector

SPCs consist of a grounded spherical metal shell filled with gas, with a high voltage ($\sim$ 2000 V) anode in its center. When a particle interacts with the gas, it converts some of its energy into

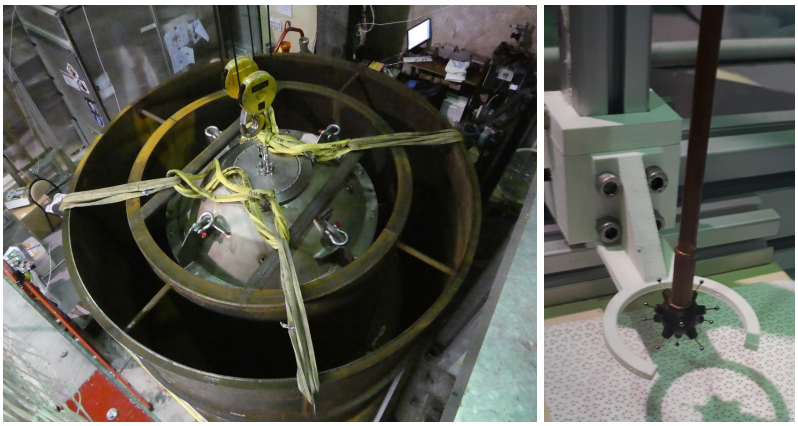

Figure 1: Left: S140 inside its lead shield, with water shield under installation, at LSM. Right: ACHINOS sensor used inside the S140.

ionization, with the resulting electrons drifting towards the central sensor, where their signal is amplified through an electronic avalanche, allowing sensitivity down to single-electron events.

The S140's shell, 140 cm in diameter, is made of C10100 copper with a 500 μm internal layer of electroplated copper [8]. Its shielding at LSM comprised a spherical lead shell, and a water shield replacing the high-density polyethylene planned for operation at SNOLAB [9], cf. Fig 1. A new multi-anode ACHINOS sensor [10] was used for its stronger electric field in the drift region. It was operated in dual-channel configuration, to keep only events happening far from the field-distortions induced by the sensor support rod, as validated by simulations [11, 12]. Detector details can be found in Ref. [6]. Ten days of data were taken with 135 mbar of CH_4 at LSM, to exploit the hydrogen sensitivity to WIMP masses down to 0.1 GeV/c^2.

3 Calibrations

The ionization quenching factor (QF) of protons between 2 and 13 keV in CH_4 was measured with a test SPC at the COMIMAC electron-and-ion generator facility in LPSC Grenoble [13]. The QF down to 510 eV was obtained by comparing the literature values of the mean ionization energy of CH_4 for electron or ion incident particles [14]. Below 510 eV, a logarithmic extrapolation ($QF(E_K) = a + b\ \ln(E_K)$, reaching a null value for nuclear recoil energies of 148 eV) was used, conservative compared to expectations from a Lindhard extrapolation.

In situ S140 calibrations included single electron events, generated by shining a 213 nm UV laser on the internal detector surface through an optical fibre feedthrough. The avalanche gain, drift and diffusion time of primary electrons were calibrated with one hour of data per day, following the procedure in Ref. [15]. To generate events uniformly in the gas volume, an ^{37}Ar source was used, producing X-rays and low-energy electrons with a total energy of 2.8 keV, 270 or 200 eV [16, 17]. Linearity of the energy response of the detector was verified, and primary electron attachment, drift and diffusion were parameterized. Together with gain calibrations performed with the UV laser, combining procedures from Ref. [15] and Ref. [18], the measured effective mean ionization energy of electronic interactions was 30 ± 0.15 eV. The Fano factor values were taken from Ref. [19] and implemented with a COM-Poisson distribution [20].

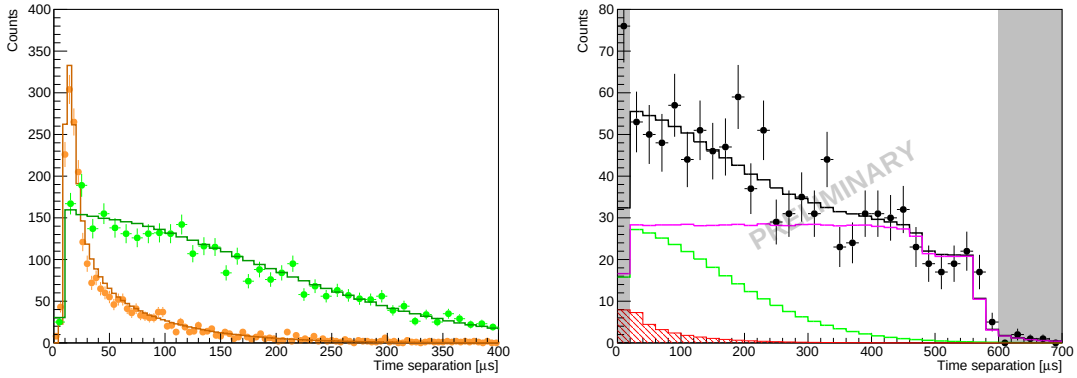

Figure 2: Time separation distribution of two-peak events. Left: Laser (green points) and ^{37}Ar (orange points) calibration data, with corresponding simulation results (green, orange curves). Right: Physics test data (black points), and best fit (black line); the green and pink lines show respectively the surface and coincidences contributions. The shaded red distribution shows the 90% confidence-level *excluded* contribution from a 0.75 GeV/c^2 WIMP. The shaded grey areas are outside the fit range.

4 Peak counting

At interaction energies under $\sim$ 200 eV$_{ee}$, producing events with few primary electrons, the Search function of ROOT's TSpectrum class [21, 22] is used to identify current spikes on the anodes with avalanches generated by the arrival of primary electrons. Events are then classified by the number of peaks founds (energy), and the time separation between first and last peak (driven by primary electron diffusion, and hence radial position) for events with at least two peaks. The UV laser calibrations show the adapted TSpectrum Search function finds 60% of single electron peaks, and distinguishes peaks 8 μs apart. Simulations of the time separation distribution of low energy events coming from either the surface or the gas volume are in good agreement with those from laser and ^{37}Ar calibrations, respectively (cf. Fig 2). The distribution for accidental coincidences was validated up to 600 μs by looking at high event rate periods in the physics data. For each peak, data quality cuts based on the rise shape of raw pulses and on the relative signal between far and near ACHINOS channels were implemented, leading to $\sim$ 95% spurious pulse rejection while keeping 77% of laser calibration events. Spurious wide pulses were observed to generate large rates of multi-peak events with short time separations, so two-peak events with time separations below 20 μs were disregarded.

5 Results

Out of ten days of physics data, 37 hours were taken to test the analysis procedure to be applied to the remaining blind data. 1086 two-peak, 180 three-peak and 131 four-peak events were recorded. A Profile Likelihood Ratio (PLR) [23] analysis was performed based on the fit of their time separation distributions, with contributions from surface and volume backgrounds, accidental coincidences, and WIMP events. The latter was based on the recoil energy spectra from Ref. [24], including the QF effect and ionization statistics described in Sec. 3.

No significant WIMP signal was observed. The best fit (cf. Fig 2) showed the observed events came predominantly from surface interactions, plus a strong contribution from accidentals with two peaks. Based on an effective exposure of 0.12 kg $\cdot$ day after quality cuts for

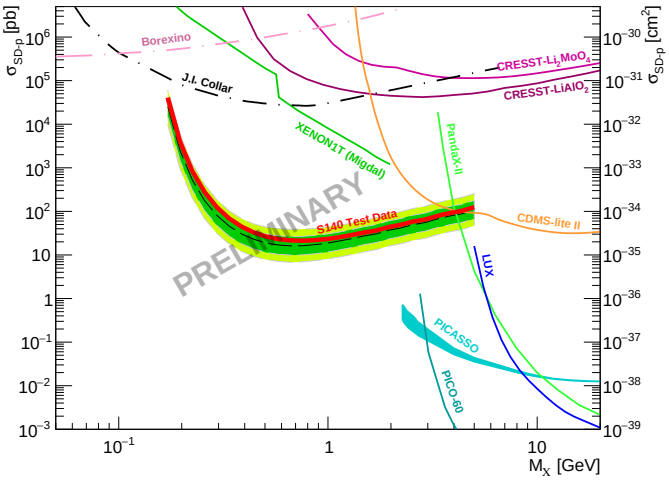

Figure 3: Preliminary spin-dependent WIMP-proton cross-section constraint from this work (red line), with median (dashed black line) and 1σ (green) and 2σ (yellow) sensitivity bands. Also shown are the existing limits from Pico-60 [25], PICASSO [26], LUX [27], PandaX-II [28], CDMS-lite II [29], CRESST-III Li_2MoO_4 [30] and $LiAlO_2$ [31] detectors, XENON1T [32], J.I. Collar [33], and Borexino [34].

the test data, preliminary constraints set on the spin-dependent WIMP-proton cross-section are world-leading in the $0.2-2\,\mathrm{GeV/c^2}$ mass range, by up to three orders of magnitude (cf. Fig 3). The remaining data, with three times more statistics, will be unblinded to produce final results after thorough review of the behaviour of the PLR in the observed background conditions.

6 Outlook

The S140 detector is currently installed at SNOLAB. Its internal surface has been etched to reduce backgrounds from impurities in the internal surface of the detector, which is expected to improve results for future physics runs taken. Mixing neon with methane will also increase the sensitivity to low energy nuclear recoils, based on SRIM [35] simulations of the QF. Beyond the current S140 detector, the Electroplated CUprum Manufacturing Experiment (ECuME) project aims to electroform a complete copper SPC for unparalleled detector radiopurity [8, 36]. A 30 cm demonstrator is under construction, with the ultimate goal being the installation in SNOLAB of an electroforming facility capable of forming a 140 cm SPC directly underground. Beyond ECuME, the proposed DarkSphere project will improve results even further with a 300 cm fully electroformed detector at Boulby Underground Laboratory. Exposure will be increased through its larger size and by running at pressures up to 5 bar, and backgrounds reduced by replacing the lead shield with a water shield.

7 Conclusion

The new S140 detector equipped with an ACHINOS sensor was operated while at LSM, producing ten days of physics data with 135 mbar of CH_4. Thanks to new calibration techniques combining a UV laser and ^{37}Ar, a detailed understanding of the detector was demonstrated, allowing analysis of data down to two-primary-electron events. The preliminary results based

on 0.12 kg · day of data show world-leading constraints on the spin-dependent WIMP-proton cross-section for WIMP masses between 0.2 and 2 GeV/c^2. Future data with the S140 at SNOLAB, and with the ECUME and DarkSphere projects, will improve even further on these results.

Acknowledgements

The help of the technical staff of the Laboratoire Souterrain de Modane is gratefully acknowledged.

Funding information This research was undertaken, in part, thanks to funding from the Canada Excellence Research Chairs Program, the Canada Foundation for Innovation, the Arthur B. McDonald Canadian Astroparticle Physics Research Institute, Canada, the French National Research Agency (ANR-15-CE31-0008), and the Natural Sciences and Engineering Research Council of Canada. This project has received support from the European Union's Horizon 2020 research and innovation programme under grant agreement No. 841261 (DarkSphere), and by UKRI-STFC through grants No. ST/V006339/1 and No. ST/S000860/1.

References

[1] P. A. Zyla et al., *Review of particle physics*, Prog. Theor. Exp. Phys. 083C01 (2020), doi:10.1093/ptep/ptaa104.

[2] D. Clowe et al., *A direct empirical proof of the existence of dark matter*, Astrophys. J. **648**, L109 (2006), doi:10.1086/508162.

[3] J. L. Feng, *Dark matter candidates from particle physics and methods of detection*, Annu. Rev. Astron. Astrophys. **48**, 495 (2010), doi:10.1146/annurev-astro-082708-101659.

[4] Q. Arnaud et al., *First results from the NEWS-G direct dark matter search experiment at the LSM*, Astropart. Phys. **97**, 54 (2018), doi:10.1016/J.ASTROPARTPHYS.2017.10.009.

[5] Q. Arnaud et al., *Solar Kaluza-Klein axion search with NEWS-G*, Phys. Rev. D **105**, 012002 (2022), doi:10.1103/PhysRevD.105.012002.

[6] L. Balogh et al., *The NEWS-G detector at SNOLAB*, J. Instrum. **18**, T02005 (2023), doi:10.1088/1748-0221/18/02/T02005.

[7] F. Piquemal, *Modane underground laboratory: Status and project*, Eur. Phys. J. Plus **127**, 110 (2012), doi:10.1140/epjp/i2012-12110-3.

[8] L. Balogh et al., *Copper electroplating for background suppression in the NEWS-G experiment*, Nucl. Instrum. Methods Phys. Res. A **988**, 164844 (2021), doi:10.1016/j.nima.2020.164844.

[9] F. Duncan, A. Noble and D. Sinclair, *The construction and anticipated science of SNOLAB*, Annu. Rev. Nucl. Part. Sci. **60**, 163 (2010), doi:10.1146/ANNUREV.NUCL.012809.104513.

[10] I. Giomataris et al., *A resistive ACHINOS multi-anode structure with DLC coating for spherical proportional counters*, J. Instrum. **15**, P11023 (2020), doi:10.1088/1748-0221/15/11/p11023.

[11] I. Katsioulas et al., *Development of a simulation framework for spherical proportional counters*, J. Instrum. **15**, C06013 (2020), doi:10.1088/1748-0221/15/06/c06013.

[12] I. Katsioulas et al., *ACHINOS: A multi-anode read-out for position reconstruction and tracking with spherical proportional counters*, J. Instrum. **17**, C08025 (2022), doi:10.1088/1748-0221/17/08/c08025.

[13] L. Balogh et al., *Measurements of the ionization efficiency of protons in methane*, Eur. Phys. J. C **82**, 1114 (2022), doi:10.1140/epjc/s10052-022-11063-9.

[14] I. Katsioulas, P. Knights and K. Nikolopoulos, *Estimation of the ionisation quenching factor in gases from W-value measurements*, Astropart. Phys. **141**, 102707 (2021), doi:10.1016/j.astropartphys.2022.102707.

[15] Q. Arnaud et al., *Precision laser-based measurements of the single electron response of spherical proportional counters for the NEWS-G light dark matter search experiment*, Phys. Rev. D **99**, 102003 (2019), doi:10.1103/PhysRevD.99.102003.

[16] V. I. Barsanov et al., *Artificial neutrino source based on the 37Ar isotope*, Phys. Atom. Nuclei **70**, 300 (2007), doi:10.1134/S1063778807020111.

[17] D. G. Kelly et al., *The production of Ar-37 using a thermal neutron reactor flux*, J. Radioanal. Nucl. Chem. **318**, 279 (2018), doi:10.1007/s10967-018-6130-8.

[18] P. Agnes et al., *Calibration of the liquid argon ionization response to low energy electronic and nuclear recoils with DarkSide-50*, Phys. Rev. D **104**, 082005 (2021), doi:10.1103/PhysRevD.104.082005.

[19] B. Grosswendt and E. Waibel, *Statistical ionisation yield fluctuations and determination of spatial ionisation and energy absorption for low energy electrons*, Radiat. Prot. Dosim. **13**, 95 (1985), doi:10.1093/rpd/13.1-4.95.

[20] D. Durnford, Q. Arnaud and G. Gerbier, *Novel approach to assess the impact of the Fano factor on the sensitivity of low-mass dark matter experiments*, Phys. Rev. D **98**, 103013 (2018), doi:10.1103/PhysRevD.98.103013.

[21] M. Morhac, *TSpectrum class reference*, https://root.cern.ch/doc/master/classTSpectrum.html.

[22] M. Morháč, J. Kliman, V. Matoušek, M. Veselský and I. Turzo, *Identification of peaks in multidimensional coincidence γ-ray spectra*, Nucl. Instrum. Methods Phys. Res. A **443**, 108 (2000), doi:10.1016/S0168-9002(99)01005-0.

[23] G. Cowan, K. Cranmer, E. Gross and O. Vitells, *Asymptotic formulae for likelihood-based tests of new physics*, Eur. Phys. J. C **71**, 1554 (2011), doi:10.1140/epjc/s10052-011-1554-0.

[24] R. Schnee, *Introduction to dark matter experiments*, in *Physics of the large and the small*, World Scientific, Singapore, ISBN 9789814327176 (2011), doi:10.1142/9789814327183_0014.

[25] C. Amole et al., *Dark matter search results from the complete exposure of the PICO-60 c_3f_8 bubble chamber*, Phys. Rev. D **100**, 022001 (2019), doi:10.1103/PhysRevD.100.022001.

[26] E. Behnke et al., *Final results of the PICASSO dark matter search experiment*, Astropart. Phys. **90**, 85 (2017), doi:10.1016/j.astropartphys.2017.02.005.

[27] D. S. Akerib et al., *Limits on spin-dependent WIMP-nucleon cross section obtained from the complete LUX exposure*, Phys. Rev. Lett. **118**, 251302 (2017), doi:10.1103/PhysRevLett.118.251302.

[28] J. Xia et al., *PandaX-II constraints on spin-dependent WIMP-nucleon effective interactions*, Phys. Lett. B **792**, 193 (2019), doi:10.1016/j.physletb.2019.02.043.

[29] R. Agnese et al., *Low-mass dark matter search with CDMSlite*, Phys. Rev. D **97**, 022002 (2018), doi:10.1103/PhysRevD.97.022002.

[30] A. H. Abdelhameed et al., *First results on sub-GeV spin-dependent dark matter interactions with ^7Li*, Eur. Phys. J. C **79**, 630 (2019), doi:10.1140/epjc/s10052-019-7126-4.

[31] G. Angloher et al., *Probing spin-dependent dark matter interactions with ^6Li*, Eur. Phys. J. C **82**, 207 (2022), doi:10.1140/epjc/s10052-022-10140-3.

[32] E. Aprile et al., *Search for light dark matter interactions enhanced by the Migdal effect or Bremsstrahlung in XENON1T*, Phys. Rev. Lett. **123**, 241803 (2019), doi:10.1103/PhysRevLett.123.241803.

[33] J. I. Collar, *Search for a nonrelativistic component in the spectrum of cosmic rays at Earth*, Phys. Rev. D **98**, 023005 (2018), doi:10.1103/PhysRevD.98.023005.

[34] T. Bringmann and M. Pospelov, *Novel direct detection constraints on light dark matter*, Phys. Rev. Lett. **122**, 171801 (2019), doi:10.1103/PhysRevLett.122.171801.

[35] J. Ziegler and J. Biersack, *SRIM (The Stopping and Range of Ions in Matter)*, Nucl. Instrum. Methods Phys. Res. B **268**, 11 (2008), doi:10.1016/j.nimb.2010.02.091.

[36] E. W. Hoppe et al., *Reduction of radioactive backgrounds in electroformed copper for ultrasensitive radiation detectors*, Nucl. Instrum. Methods Phys. Res. A **764**, 116 (2014), doi:10.1016/j.nima.2014.06.082.